DAMAGE EFFECT ON THE NONLINEAR DYNAMIC RESPONSE OF A BRIDGE

Thiago de Oliveira Abeche[1]

Roberto Dalledone Machado[2]

João Elias Abdalla Filho[3]

t.abeche@gmail.com[1]

roberto.machado@pucpr.br[2]

joao.filho@pucpr.br[3]

Mechanical Engineering Graduate Program, Pontifical Catholic University of Paraná (PUCPR)[123]

Imaculada Conceição Street 1155, 80215-901, Curitiba, Paraná, Brazil[123]

Numerical Methods in Engineering Graduate Program, Federal University of Paraná (UFPR)[2]

Cel. Francisco Heráclito dos Santos Street 210, 81531-990, Curitiba, Paraná, Brazil[2]

Fernando Luiz Martinechen Beghetto[4]

Luiz Antonio Farani de Souza[5]

flbeghetto@utfpr.edu.br[4]

lasouza@utfpr.edu.br[5]

Federal Technological University of Paraná (UTFPR)[345]

Deputado Heitor Alencar Furtado Street 4900, 81280-340, Curitiba, Paraná, Brazil[34]

Marcílio Dias Street 635, 86812-460, Apucarana, Paraná, Brazil[5]

Abstract. *The constant movement of vehicles on bridges can, over time, affect the structural integrity and compromise its service life. The lack of supervision allows overloads that can damage the pavement and the bridge. The lack of maintenance and conservation of the structures do not guarantee safety and structural health. When crossing a bridge with constant speed, the vehicle is subjected to the effects of track irregularities, represented by sinusoidal harmonic functions. The irregularities of the track dynamically excite the vehicle which in turns provokes additional vibrations in the structure of the bridge beyond those produced by their own movement, increasing the degree of damage of the structure. The approach developed in this study treats this phenomenon uncoupled. The damage modifies the dynamic responses of the bridge structure, increasing the magnitude and the oscillations within the same time interval especially at critical speeds of the vehicle, capable to provoke* *some resonance. Apart from changing the responses in terms of displacements, velocities and accelerations, the damage alters the natural frequencies of vibration of the structure. Such effects are not possible to be analyzed with linear dynamic models. In this sense, this work aims to evaluate the nonlinear dynamic effects produced in a reinforced concrete bridge through the Finite Element Method, on which the degree of damage is altered over time through the stiffness loss of the structure by Damage Mechanics. The damage model used is the Mazars Damage Constitutive Model implemented with the condition of stress inversion due to vibration. In the bridge model are used Euler-Bernoulli beam elements, with Hermite cubic interpolation functions. The structural damping is defined by the Rayleigh method with the updated coefficients. Effects of nonlinearities occur by the fact that the forces no longer linearly depend from the displacements when damage occurs. The continuum damage mechanics is considered dynamically, requiring to evaluate the damage in each layer of the structure section for each iteration within each time step. In this way, the equations of motion are obtained by nonlinear dynamic equilibrium and numerically integrated in time using the Newmark Method together with the Newton-Raphson iterative Method. This proposal seeks to contribute to the study of the health monitoring of bridges structures on which the lack of supervision and maintenance affect the structural integrity.*

Keywords: *Damage Mechanics, Dynamic Interaction, Finite Element Method, Computational Modeling*

1 INTRODUCTION

The increase in road and railroad transport cargo, especially in Brazil, with increased intensity values of loads on the roads, has been producing degradation in many bridges throughout the countries. This is an issue of paramount importance, as is related to the structural health of bridges and with the matter of the conservation of roads and railway structures (Abeche et al., 2015).

Often, specialized consultants are held in the design and dimensioning of more complex structures such as bridges, dams and nuclear reactors in order to ensure the proper behavior of the structure before effects that may not be well represented with a common analysis.

For safety established by technical rules, such structures need to be evaluated before more stringent criteria to ensure structural integrity. In many cases, nonlinear effects are verified on structures even if they have predominantly linear behavior. At the same time, in many problems it is necessary to dynamically analyze the nonlinearities on these structures.

Other factor is due to the emergence of new and complex structural systems, subjected to preponderantly dynamic actions. This is the case, for example, of offshore structures, oil exploration and exploitation in the continental offshore. The dynamic analysis of these structures is fundamental because one of the most important loads to be considered in the project is due to wave action (Machado, 1983).

The impossibility of the exact solution of a physical phenomenon is due to the complex nature of differential equations, but may also be given to initial problems or even boundary conditions. The engineering experiences that in many practical cases where it is not always possible to reach analytical solution or the idealization of the perfect solution. Therefore, the engineering uses numerical approximations that interpolate exact values calculated at a specific number of points seeking a more accurate response for the real solution.

However, not always an improvement in the degree of refinement of the analysis approaches the analytical solution effectively, approaching the solution tangentially. After this limit, if there is an even greater increase in the number of analysis, there may be a greater computational effort for a few gains in approach and, in some cases, the obtained response can even differ from the analytical solution.

In such cases, to have a greater gain in numerical solution, it is necessary to analyze the problem with more theories, including them in order to consider greater truths in the problem, as occur with dynamic approach, in which one can perceive an increase of the displacements before the static displacements in most cases.

In this sense, are being studied the problems of dynamic interaction between vehicle and bridge considering the track irregularities. There are numerous references in the literature dealing with this topic and the modeling of vehicle-bridge systems considering track irregularities has been studied by many researchers around the world in the last thirty years.

This work seeks to contribute to these studies of health monitoring of bridges and structural integrity by analyzing the damage effect on the nonlinear dynamic responses of bridges.

2 MATHEMATICAL MODEL OF VEHICLES COUPLED WITH IRREGULARITIES

This implemented computational model considers the passage of the vehicle with one degree of freedom in the different forms of track irregularities and transmits the stresses generated between the vehicle and irregularities to the bridge, in uncoupled way, for its dynamic linear or nonlinear analysis. In other words, the dynamic responses of the bridge do not affect the forces caused by the coupling between the passing vehicle and irregularities. Thus, this computational routine firstly analyzes the forces generated by the coupling between vehicle and irregularities and transmits them to the bridge for the desired analysis. Therefore, it is a model coupled between vehicle and irregularities and uncoupled between the coupled vehicle-irregularities and the bridge.

The model with 1 degree of freedom consists of a wheel mass m_1 in contact with the irregularities, a suspended vehicle mass m_2, a spring with stiffness coefficient k and a damper with damping coefficient c, as showed in Figure 1.

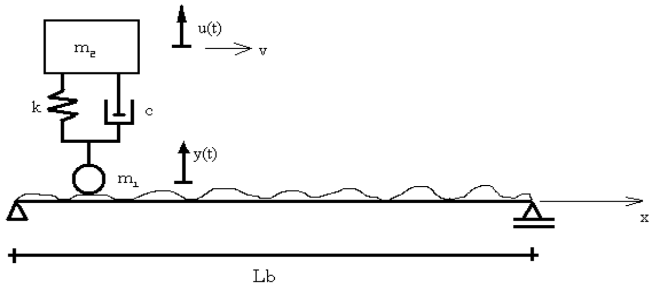

Figure 1. Vehicle-irregularities model with 1 degree of freedom

When crossing a bridge with speed v, the vehicle is subjected to the effects of track irregularities, represented by $y(t)$. Considering the wheel mass undeformable, this is similar to a case of base excitation. It is merely necessary to consider the vehicle stationary subjected to a harmonic base excitation $y(t)$. The spring and the dumper masses are neglected throughout the analysis. Assuming a linear elastic behavior for the spring and a linear viscous damping for the damper throughout the analysis, the elastic force acting on the spring and the damping force are

$$f_M = k[u_v(t) - y(t)] \tag{1}$$

$$f_A = c[\dot{u}_v(t) - \dot{y}(t)] \tag{2}$$

Thus, the governing equation of motion of the problem can be written as

$$m_2\ddot{u}_v(t) + c[\dot{u}_v(t) - \dot{y}(t)] + k[u_v(t) - y(t)] = 0 \tag{3}$$

In Table 1 are illustrated the following forms of track irregularities

Table 1. Forms of track irregularities

Sinusoidal harmonic	Triangular periodic	Rectangular periodic
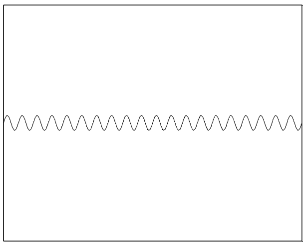	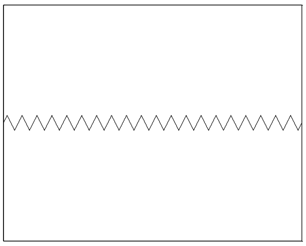	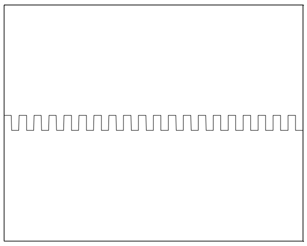

For each irregularity described in Table 1 are determined the different vehicle-irregularities coupled models.

In each base excitation function $y(t)$ that represents each type of track irregularities, the function is derivate with respect to time to obtain the portion $\dot{y}(t)$ related to the resistive force due to damping

$$\dot{y}(t) = \frac{dy(t)}{dt} \tag{4}$$

The numerical differentiation is used analyzing the accuracy in most of the described cases or when the analyzed irregularities are random.

Considering v as the vehicle speed, l the wave length of the irregularities, t the time and A the amplitude, the irregularities functions to the sinusoidal harmonic case can be expressed as

$$y(t) = A\sin\left(\frac{2\pi v}{l}t\right) \tag{5}$$

The Eq. (5) represents the irregularities of the track in the form of a sinusoidal harmonic function correlated with the vehicle speed. If deriving Eq. (5) with respect to time, it has

$$\dot{y}(t) = \frac{2\pi A v}{l}\cos\left(\frac{2\pi v}{l}t\right) \tag{6}$$

By replacing Eq. (5) and Eq. (6) in Eq. (3), one obtains

$$m_2\ddot{u}_v(t)+c\dot{u}_v(t)+ku_v(t)=c\left[\frac{2\pi Av}{l}\cos\left(\frac{2\pi v}{l}t\right)\right]+k\left[A\sin\left(\frac{2\pi v}{l}t\right)\right] \tag{7}$$

The force produced by the base excitation is defined by

$$F_{EB}(t)=(m_1+m_2)g+c[\dot{u}_v(t)-\dot{y}(t)]+k[u_v(t)-y(t)] \tag{8}$$

where g is the acceleration of gravity.

3 LINEAR DYNAMIC MATHEMATICAL MODEL OF THE RAILWAY BRIDGE

In this model, as Yang, Yau and Hsu (1997), no distinction is made for the geometry of the bridge cross section, analyzing the problem with only the moment of inertia.

The supported bridge shown in Figure 1 has constant cross section and stiffness along its length L_b. As can be seen in classical literature (Chopra, 1995; Bathe, 1996; Kwon & Bang, 2000), for the Euler-Bernoulli beam finite element used in this model, the elementary matrices of stiffness and mass are given respectively by

$$[K_e]=\frac{EI}{L^3}\begin{bmatrix}12 & 6L & -12 & 6L\\ 6L & 4L^2 & -6L & 2L^2\\ -12 & -6L & 12 & -6L\\ 6L & 2L^2 & -6L & 4L^2\end{bmatrix} \tag{9}$$

$$[M_e]=\frac{\rho AL}{420}\begin{bmatrix}156 & 22L & 54 & -13L\\ 22L & 4L^2 & 13L & -3L^2\\ 54 & 13L & 156 & -22L\\ -13L & -3L^2 & -22L & 4L^2\end{bmatrix} \tag{10}$$

In Equation (9) and Equation (10), the physical parameters E and ρ are, respectively, the elastic modulus and the linear mass density of the element, whereas geometric parameters A, I and L, represent respectively the cross-sectional area, the moment of inertia and the length of the element.

The equation of dynamic forces on each element is defined by

$$\{F_e(t)\}=\int_0^L q(x,t)[H]^T\,dx \tag{11}$$

where $[H]$ contains the cubic Hermite interpolation functions, like

$$[H]=\begin{bmatrix}1-3(x/L)^2+2(x/L)^3\\ x\left[1-2(x/L)+(x/L)^2\right]\\ 3(x/L)^2-2(x/L)^3\\ x\left[(x/L)^2-(x/L)\right]\end{bmatrix} \tag{12}$$

where x is the abscissa in which are located the efforts in each element and L the element length.

Substituting Eq. (8) in Eq. (11) and integrating, the elementary external force vector $\{F_e(t)\}$ is defined by

$$\{F_e(t)\} = -F_{EB}(t)[H] \tag{13}$$

wherein the negative sign is assigned due to the convention system defined previously.

The abscissa x is set as function of time t and velocity v, thereby the Eq. (12) becomes

$$[H^*] = \begin{bmatrix} 1-3(vt/L)^2+2(vt/L)^3 \\ vt\left[1-2(vt/L)+(vt/L)^2\right] \\ 3(vt/L)^2-2(vt/L)^3 \\ vt\left[(vt/L)^2-(vt/L)\right] \end{bmatrix} \tag{14}$$

Rewriting the Eq. (13) using the Eq. (14), we obtain

$$\{F_e(t)\} = -F_{EB}(t)[H^*] \tag{15}$$

Defined the elementary matrices of stiffness and mass and the elementary external force vector, the global matrices of the undamaged bridge structure are assembled through the connectivity of each element. Using the Rayleigh method for the structural damping, the global equation of motion for the without considering the geometry of the bridge's cross section is written as

$$[M_B]\{\ddot{u}_B\}+[C_B]\{\dot{u}_B\}+[K_B]\{u_B\}=\{F_B(t)\} \tag{16}$$

where $[M_B]$, $[C_B]$ and $[K_B]$ are the global matrices of mass, damping and stiffness, $\{u_B\}$, $\{\dot{u}_B\}$ and $\{\ddot{u}_B\}$ are the global vectors of displacement, velocity and acceleration, and $\{F_B(t)\}$ is the external force vector. Here, the Newmark method is utilized with average acceleration to time integration of Eq. (16), and the system is solved by Gaussian elimination method.

So far, the responses of the bridge are obtained by linear dynamic analysis without considering the geometry of the cross section. However, in a case of deterioration of the material, the forces are no longer linearly dependent of the displacements. This work considers that the damage affect the stiffness of the system, causing the previously fixed stiffness matrix to become instantaneous, characterizing physical nonlinearity, as shown below

$$[K_B]=[K_B(u_B)] \tag{17}$$

To be able to perform an adequate nonlinear dynamic analysis, firstly it is need to better understand how the damage mechanics affects the stiffness of the system. While the fracture mechanics works with the condition of macroscopic cracks propagation, the damage mechanics studies the distributed microscopic crack effect on the response of the material. This paper considers the damage mechanics in the concrete, a material in which the micro cracking is the dominant phenomenon in nonlinear behavior, starting already during the concrete curing in a distributed way even with low stresses and deformations and even before any load application. In this sense, it is presented the Mazars damage constitutive model below.

4 MAZARS DAMAGE CONSTITUTIVE MODEL

Rabotnov (1969) proposed to consider the loss of material stiffness as a result of cracking. Posteriorly, the continuum damage mechanics was formalized based on thermodynamics of irreversible processes by Lemaitre & Chaboche (1985).

The damage evolution in the concrete is simulated with the damage constitutive model proposed by Mazars (1984). This model is based on some experimental evidences observed in uniaxial experiments in concrete, having the fundamental hypotheses (Pituba, 1998):

– the damage is represented by a scalar variable D $(0 \le D \le 1)$ whose evolution occurs when a reference value for the 'equivalent stretching' is exceeded;

– locally the damage comes from the existence of stretching deformations;

– its considered, that the damage is isotropic, although experimental tests show that the damage leads, in general, to an anisotropy of concrete (which may initially be considered as isotropic); and

– the damaged concrete behaves as an elastic medium, therefore the permanent deformation evidenced experimentally in a situation of unloading is neglected.

The square of the equivalent strain is equal to the sum of the squares of the main components of the positive principal strain

$$\tilde{\varepsilon}^2 = \sum_i \left\langle \varepsilon_i^2 \right\rangle_+ \qquad (i = 1,2,3,\ldots,\infty) \tag{18}$$

The extension state is locally characterized by a stretching or an equivalent strain, expressed as (Pituba, 1998)

$$\tilde{\varepsilon} = \sqrt{\left\langle \varepsilon_1 \right\rangle_+^2 + \left\langle \varepsilon_2 \right\rangle_+^2 + \left\langle \varepsilon_3 \right\rangle_+^2 + \ldots + \left\langle \varepsilon_n \right\rangle_+^2} \qquad (i = 1,2,3,\ldots,\infty) \tag{19}$$

where ε_i are the principal strain components and $\left\langle \varepsilon_i \right\rangle_+$ its positive parts defined by

$$\left\langle \varepsilon_i \right\rangle_+ = \frac{1}{2}\left[\varepsilon_i + |\varepsilon_i|\right] \tag{20}$$

In this model, is adopted that the damage starts when the equivalent strain $\tilde{\varepsilon}$ reaches a value of the reference strain ε_{d0} determined in uniaxial traction tests in correspondence to the maximum stress, as the following Figure 2.

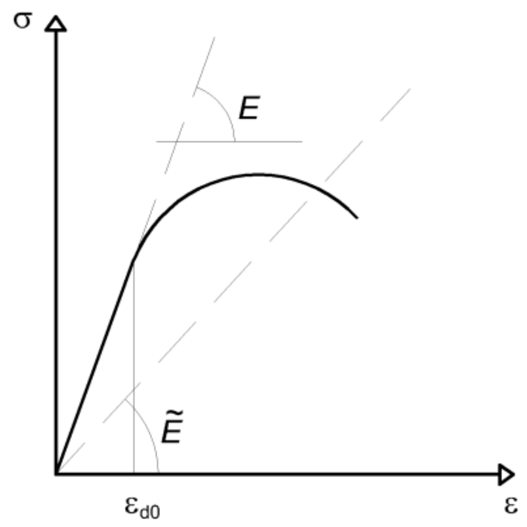

Figure 2. Stress-strain diagram for Mazars damage constitutive model

The constitutive relation, for the particular case of unidimensional stress state, is given by (Tiago et al., 2002)

$$\sigma = (1 - D(\varepsilon))E_{c0}\varepsilon \tag{21}$$

in which E_{c0} being the initial elastic modulus, that is, of the non-damaged material.

The damage variable D is defined by a linear combination of the basic damage variables D_T and D_C through the combination coefficients α_T and α_C by

$$D(\varepsilon) = \alpha_T D_T + \alpha_C D_C \qquad \alpha_T + \alpha_C = 1 \tag{22}$$

in which the value of the coefficients α_T and α_C are contained in the closed interval $[0,1]$, and seek to represent the contribution of the mechanical requests to traction and compression for the extension local state, respectively (Pituba & Proença, 2005).

The basic damage variables are given by

$$D_T(\tilde{\varepsilon}) = 1 - \frac{\varepsilon_{d0}(1 - A_T)}{\tilde{\varepsilon}} - \frac{A_T}{e^{B_T(\tilde{\varepsilon} - \varepsilon_{d0})}} \tag{23}$$

and

$$D_C(\tilde{\varepsilon}) = 1 - \frac{\varepsilon_{d0}(1 - A_C)}{\tilde{\varepsilon}} - \frac{A_C}{e^{B_C(\tilde{\varepsilon} - \varepsilon_{d0})}} \tag{24}$$

where A_T, B_T, A_C and B_C are the characteristic parameters of the material in uniaxial traction and uniaxial compression, respectively, $\tilde{\varepsilon}$ the equivalent strain below which no damage occurs and ε_{d0} the parameter of the limit elastic deformation. The subscripts T and C refer to traction and compression, respectively. Therefore, if the equivalent strain is lesser then the reference strain $(|\tilde{\varepsilon}| < \varepsilon_{d0})$, then there is no damage at all $(D = 0)$.

In order to consider the poisson effect in the concrete, the equivalent strain is given by

$$\tilde{\varepsilon} = \begin{cases} \varepsilon, & if\ \varepsilon \geq 0 \\ -\nu\sqrt{2}\varepsilon, & otherwhise \end{cases} \tag{25}$$

where ν is the Poisson's ratio of the concrete.

Mazars (1984) proposed the following ranges of variation for the parameters A_T, B_T, A_C and B_C, obtained from the calibration with experimental results (Pituba, 1998)

$$\begin{array}{lll} 0{,}7 \leq A_T \leq 1 & 10^4 \leq B_T \leq 10^5 & 10^{-5} \leq \varepsilon_{d0} \leq 10^{-4} \\ 1 \leq A_C \leq 1{,}5 & 10^3 \leq B_C \leq 2.10^3 & \end{array} \tag{26}$$

The Figure 3 shows the behavior of the Mazars damage model when the material is subjected to traction and compression.

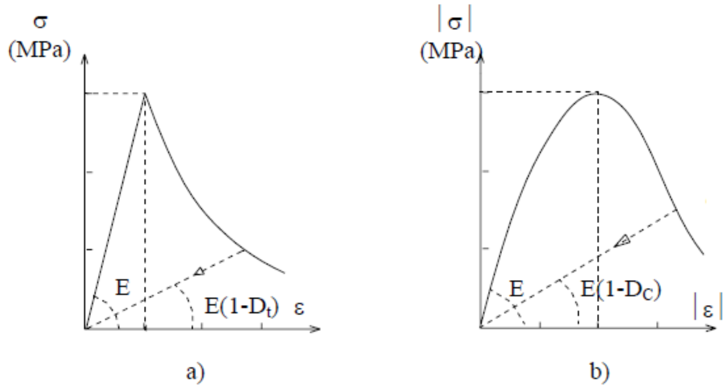

Figure 3. Uniaxial response of Mazars model: (a) traction, (b) compression (adapted from Pituba, 1998)

A more rigorous way to define the damage is through the fourth order damage tensor D_{ijrs} considering the operator that transforms the initial elasticity tensor of the intact material E_{ijkl} in the current elasticity tensor of the material softened by damage $\tilde{E}_{ijkl}$ by

$$\tilde{E}_{ijkl} = \left(I_{ijrs} - D_{ijrs}\right)E_{rskl} \tag{27}$$

From a purely theoretical point of view, the relationship shown above in Eq. (27) does not produce a real state variable because it requires knowledge of a particular behavior of the material, such as elasticity (Lemaitre & Desmorat, 2005). However, this relationship allows to indirectly determining the damage variable for elastic materials from Young's modulus measurements performed in tests with loading and unloading cycles.

In the case of uniaxial isotropic damage without the effect of micro cracks closure in compression, the average value of micro stresses is obtained from the equilibrium of forces (Rabotnov, 1969). Thus, the effective stress $\tilde{\sigma}$ can be written as

$$\tilde{\sigma} = \frac{F}{\tilde{S}} = \frac{F}{S(1-D)} = \frac{\sigma}{(1-D)} \tag{28}$$

where F is the applied force in the representative volume element, $\tilde{S}$ is the effective area which is the intact area S subtracted by the defects area SD, and σ is the stress acting on the intact area.

The state of deformation one-dimensional or three-dimensional of a damaged material is obtained by the behavior of the intact material where the stress is replaced by the effective stress (Lemaitre & Chaboche, 1985). Therefore the equivalent deformation ε_e can be defined by

$$\varepsilon_e = \frac{\tilde{\sigma}}{E} = \frac{\sigma}{(1-D)E} \tag{29}$$

in which E is the Young's modulus of the intact material.

Thus, the Young's modulus of the damaged material $\tilde{E}$ for a continuous medium with equivalent response to the material with imperfections is obtained by

$$\tilde{E} = (1-D)E \tag{30}$$

Although the Mazars damage constitutive model considers that the damaged concrete behaves as an elastic medium, despising the permanent deformation in unloading situations, the damage is irreversible and cumulative. In this way, if the load is removed from the damaged material the Young's modulus E is updated to the damaged Young's modulus $\tilde{E}$ and does not return to its initial state, it can only be more damaged.

5 CONSTITUTIVE MODEL FOR THE STRUCTURAL STEEL

For the structural steel, it is adopted a bilinear elastoplastic model with strain hardening having the same behavior when subjected to traction and compression. As in reinforced concrete structures the steel bars resist fundamentally the axial forces, it is used an uniaxial model to describe the behavior of the reinforcement. The Figure 4 shows a bilinear stress-strain diagram with strain hardening for the structural steel (Pasa, 2007).

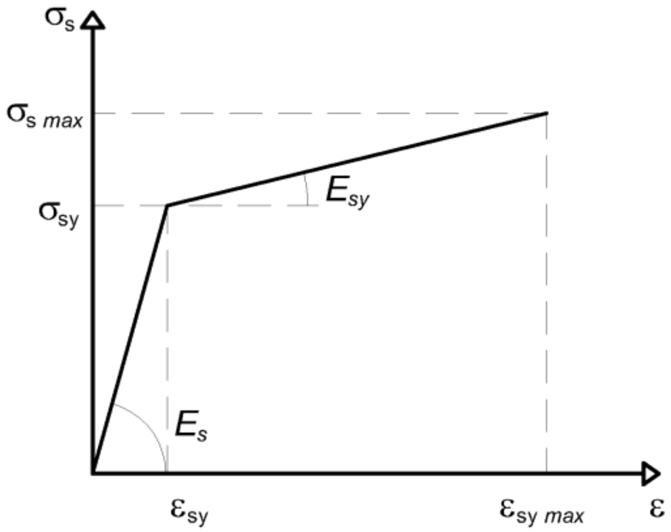

Figure 4. Bilinear elastoplastic model with strain hardening for the structural steel

In this model, if the structural steel is unloaded at the second section of the diagram shown above, the model has a permanent deformation associated.

That way, the stress acting on the structural steel is determined by (Tiago et al., 2002)

$$\sigma = \begin{cases} E_s \varepsilon, & -\varepsilon_{sy} \le \varepsilon \le \varepsilon_{sy} \\ E_{sy} \varepsilon, & otherwhise \end{cases} \tag{31}$$

where E_s is the initial elastic modulus of the structural steel, ε_{sy} is the yield extension and E_{sy} is the longitudinal elastic modulus after the yield of the steel defined by

$$E_{sy} = k_s E_s \tag{32}$$

wherein k_s is the relation between the longitudinal elastic modulus after the yield of the steel E_{sy} and the longitudinal elastic modulus of the steel E_s.

6 EQUIVALENT STIFFNESS

The continuum damage mechanics is considered dynamically. In this sense, it is necessary to evaluate the damage in each cross section of the bridge's elements, for each iteration within each time steps.

The rectangular cross section of the bridge's elements are divided in n layers as laminated composite beams in order to be able to determine the equivalent stiffness of each element, as shown in Figure 5.

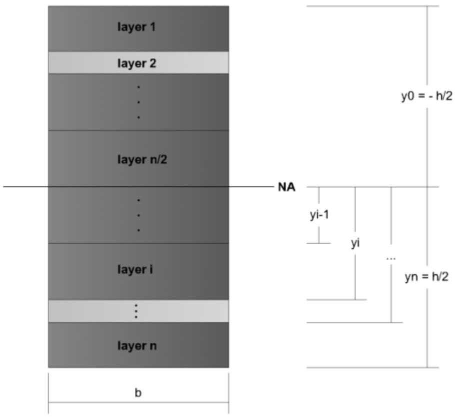

Figure 5. Rectangular cross section of the bridge's elements divided into layers

For a particular case of symmetric laminated composite beam with b width, the equivalent stiffness EI_{eqv} is determined by

$$EI_{eqv} = \frac{1}{3} b \sum_{i=1}^{n} E_i \left(y_i^3 - y_{i-1}^3 \right) \tag{33}$$

where n is the number of layers, b is the constant width of the rectangular cross section, E_i is the elastic modulus of the i^{th} layer, in the case E_c for the concrete layers and E_s for the layers representing the structural steel, y_i and y_{i-1} are the y axis coordinate values of the division points of the i^{th} which subtracted result in the height of the layer.

In obtaining the elementary internal force vector, the equivalent bending stiffness is determined for each Gauss point in the numerical integration by using the Gaussian quadrature method.

In the calculation process of the equivalent stiffness, when the materials, concrete or structural steel, present nonlinear behavior, the position of the neutral axis varies and is recalculated at each numerical iteration according to the deterioration of any layer by

$$y_{NA} = \frac{\sum \frac{(y_i - y_{i-1})}{2} E_i A_i}{\sum E_i A_i} \tag{34}$$

where A_i is the area of the layer and y_{NA} is the recalculated position of the neutral axis.

7 NONLINEAR DYNAMIC MATHEMATICAL MODEL THROUGH DAMAGE MECHANICS FOR THE BRIDGE

After reviewing the Mazars damage model, the constitutive model for the structural steel and the equivalent stiffness model, this nonlinear dynamic model considers the geometry of the bridge's cross section in order to locate damages in each layer of each element for each iteration within each time step.

As explained in Eq. (17), due to Eq. (30), the global equation of motion of the damaged bridge is written as (Jacob & Ebecken, 1994)

$$[M_B]_{t+\Delta t}^{(i-1)} \{\ddot{u}_B\}_{t+\Delta t}^{(i)} + [C_B]_{t+\Delta t}^{(i-1)} \{\dot{u}_B\}_{t+\Delta t}^{(i)} + [K_B]_{t+\Delta t}^{(i-1)} \{\Delta u\}^{(i)} = \{F_B^{ext}\}_{t+\Delta t} - \{F_B^{\text{int}}(\{u_B\}_{t+\Delta t}^{(i-1)})\}_{t+\Delta t}^{(i-1)} \tag{35}$$

The above nonlinear Eq. (35) of motion is solved in incremental and iterative way by the combination of the modified Newton-Raphson iterative technique with the implicit time integration operator of the Newmark method. Using the Newmark coefficients, the global equation of motion becomes

$$\begin{aligned}
&\left(\frac{[M]_{t+\Delta t}^{(i-1)}}{\alpha \Delta t^2} + \frac{\delta [C]_{t+\Delta t}^{(i-1)}}{\alpha \Delta t}\right)\{u_B\}_{t+\Delta t}^{(i)} + [K_B]_{t+\Delta t}^{(i-1)}\{\Delta u\}^{(i)} = \\
&\underset{\sim}{F}{}_{t+\Delta t}^{ext} + \frac{[M]_{t+\Delta t}^{(i-1)}}{\alpha \Delta t^2}\left(\{u_B\}_t + \{\dot{u}_B\}_t \Delta t + (0.5-\alpha)\{\ddot{u}_B\}_t \Delta t^2\right)^{(i)} \\
&+ [C]_{t+\Delta t}^{(i-1)}\left(\frac{\delta}{\alpha \Delta t}\{u_B\}_t + \left(\frac{\delta}{\alpha} - 1\right)\{\dot{u}_B\}_t + \left(\frac{\delta}{2\alpha} - 1\right)\{\ddot{u}_B\}_t \Delta t\right)^{(i)} - \{F_B^{\text{int}}\}_{t+\Delta t}^{(i-1)}
\end{aligned} \tag{36}$$

or

$$[M_B]_{t+\Delta t}^{(i-1)} \{\ddot{u}_B\}_{t+\Delta t}^{(i)} + [C_B]_{t+\Delta t}^{(i-1)} \{\dot{u}_B\}_{t+\Delta t}^{(i)} + [K_B]_{t+\Delta t}^{(i-1)} \{\Delta u\}^{(i)} = \{\Delta F_B\}_{t+\Delta t} \tag{37}$$

where

$$\{\Delta F_B\}_{t+\Delta t} = \{F_B^{ext}\}_{t+\Delta t} - \{F_B^{\text{int}}\}_{t+\Delta t}^{(i-1)} \tag{38}$$

The first values of displacement and velocity are estimated, in iterative way, through the predictive values of displacement and velocity defined as (Machado, 1983)

$$\{u\}_{t+\Delta t}^{(i)} = \{\tilde{u}\}_{t+\Delta t} \tag{39}$$

and

$$\{\dot{u}\}_{t+\Delta t}^{(i)} = \{\tilde{\dot{u}}\}_{t+\Delta t} \tag{40}$$

where (i) is the iteration number within each time step.

The internal global force seeks the nonlinear dynamic equilibrium configuration. Its components are the forces parcels from the stresses acting in each of the layers of the cross section for each element. These are obtained at each iteration within each time step as (Bathe, 1996)

$$\{F_B^{\text{int}}\}_{t+\Delta t}^{(i-1)} = \sum_m \int_{V_{t+\Delta t}^{(m)}} [B]_{t+\Delta t}^{(m)\,T} [\sigma]_{t+\Delta t}^{(m)} dV_{t+\Delta t}^{(m)} \tag{41}$$

The convergence is acquired to an energy criteria that includes both forces and displacements criteria, as (Idem, 1996)

$$\{\Delta u\}^{(i)T}\left(\{R\}_{t+\Delta t} - \{F\}_{t+\Delta t}^{(i-1)}\right) \leq \varepsilon_E \left(\{\Delta u\}^{(1)T}\left(\{R\}_{t+\Delta t} - \{F\}_t\right)\right) \tag{42}$$

8 NUMERICAL ANALYSIS

The following Table 2 illustrates the input data used in the analysis.

Table 2. Input data

Input Data			
Vehicle	Irregularities	Bridge	Damage Parameters
$m_1 = 4.400\ kgf$	$y_1 = A\sin(\omega_e t)$	$L_b = 20\ m$	$A_T = 0{,}995$
$m_2 = 17.600\ kgf$	$y_2 = Atri(\omega_e t)$	$b = 0{,}4\ m$	$B_T = 30.000$
$k = 9.120\ kN/m$	$y_3 = Arect(\omega_e t)$	$h = 3{,}9494\ m$	$A_C = 1{,}2$
$c = 96\ kNs/m$	$A = 0{,}005\ m$	$I = 3{,}81\ m^4$	$B_C = 1.050$
$v = 30\ km/h$	$L = 0{,}2\ m$	$m = 34{,}088\ kg/m$	$\varepsilon_{d0} = 10^{-4}$
$\omega_n = 143{,}0280\ rad/s$	$\omega_e = 87{,}2665\ rad/s$	$\omega_{n1} = 44{,}75\ rad/s$	
2.000 *Time Steps*	$\omega_n = 143{,}0280\ rad/s$	$E_c = 29{,}43\ GPa$	
	2.000 *Time Steps*	$\nu_c = 0{,}2$	
		$E_s = 210\ GPa$	
		$\nu_s = 0{,}3$	
		$k_s = 0{,}85$	
		60 *Layers*	
		$\zeta = 0{,}025$	
		20 *Elements*	
		10.000 *Time Steps*	
		Newmark $(0{,}5\ e\ 0{,}25)$	
		Supported bridge	

where the $y_1 = A\sin(\omega_e t)$, the $y_2 = Atri(\omega_e t)$ and the $y_3 = Arect(\omega_e t)$ represent, respectively, the sinusoidal harmonic, triangular periodic and rectangular periodic forms of irregularities presented in Table 1.

The Figure 6 shows the static and dynamic responses of displacement for the sinusoidal, triangular and rectangular forms of irregularities obtained with the linear dynamic routine without the consideration of the geometry of the bridge's cross section, just considering the moment of inertia. The moment of inertia is considered constant along the length of the bridge as, in this model, no damage occurs.

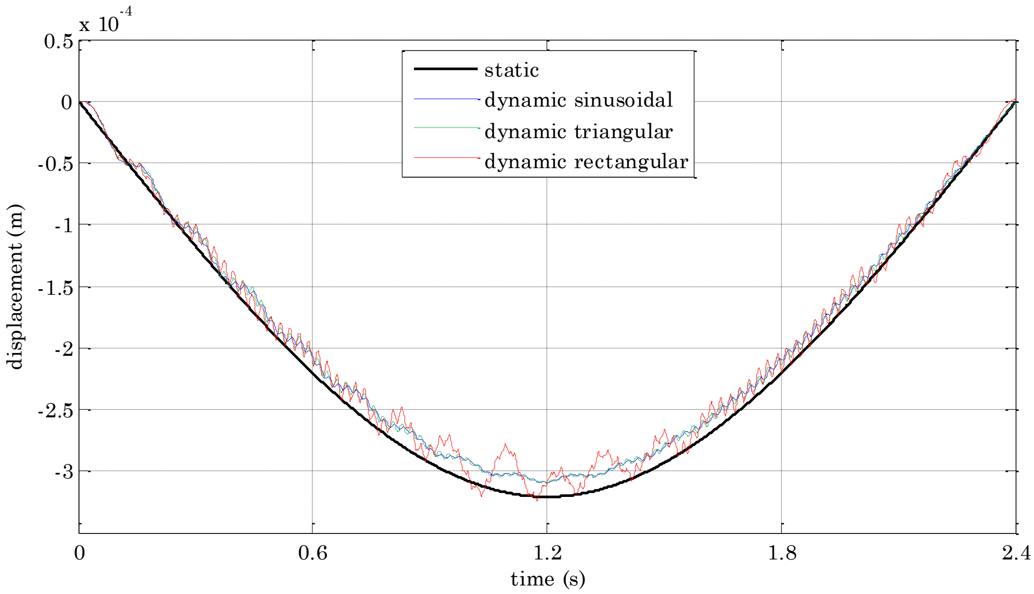

Figure 6. Displacement responses in the mid-span without considering geometry of the cross section

It is noted that the dynamic responses obtained with the routine that does not considers the geometry of the cross section does not oscillate around the static response, standing beneath it. That is why this routine is not reliable to represent the dynamic responses for the exemplified case. However, this model is still effective in some cases. The wavelength chosen in this analysis was sufficiently small in order to make this routine unable to represent the real responses of the structure. Although not the case, this model also cannot represent the real responses in cases of extremely high loads. For this reason, the article will not show the obtained dynamic responses of velocity and acceleration with this routine.

Next, all the graphics shown are obtained with the second routine capable to capture the effects of nonlinearities caused by damage, considering the geometry of the bridge's cross section. If no damage occurs, the responses turn to be linear dynamics considering these geometries, unlike the first routine. And in case of any damage, the routine is able to capture them turning the response to nonlinear dynamics considering the geometries of the bridge.

The Figure 7 shows the static and dynamic responses of displacement with the second routine.

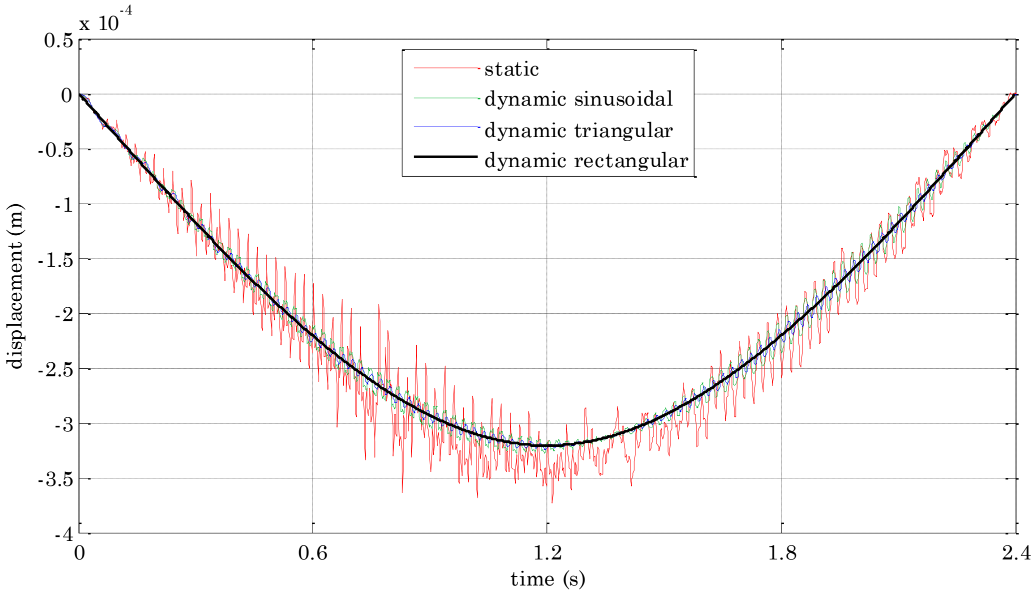

Figure 7. Displacement responses in the middle of the span with

It can be observed that the dynamic responses of displacement for the different cases of irregularities now oscillate around the static response, being a more reliable response. The track irregularities associated with the vehicle vibrations caused greater oscillations in dynamic displacement responses. Naturally, the displacements obtained from the rectangular irregularities are greatly then all the others, but it was much more amplified because these irregularities were able to cause damage to the material. After the rectangular irregularities, the triangular irregularities were more intensified than the sinusoidal.

The Figure 8 shows the effect of structural damping on the dynamic responses of displacement.

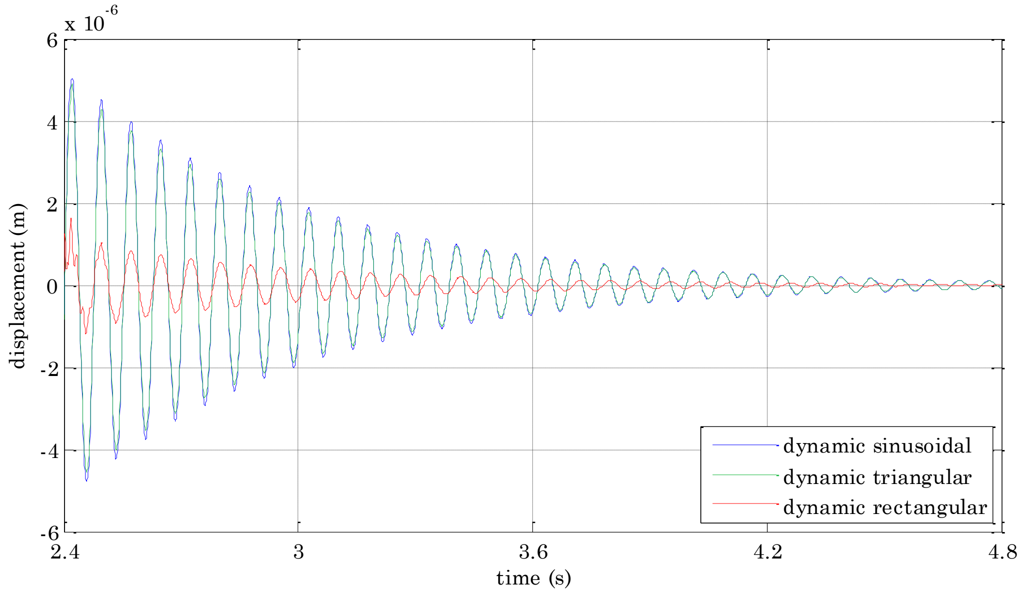

Figure 8. Effect of the structural damping on the dynamic responses of the mid-span displacement

It can be observed that the rectangular dynamic responses of displacements, which were more prejudicial to the structure, are more easily damped followed by the triangular and sinusoidal dynamic responses of displacement. In other words, the greatest impact responses are more easily damped.

As any dynamic analysis, the structure will have responses in terms of velocities and accelerations. The damage mechanics clearly affects these responses since the Young's modulus is altered over time.

The Figure 9 presents the dynamic responses of velocity to sinusoidal, triangular and rectangular forms of periodic irregularities.

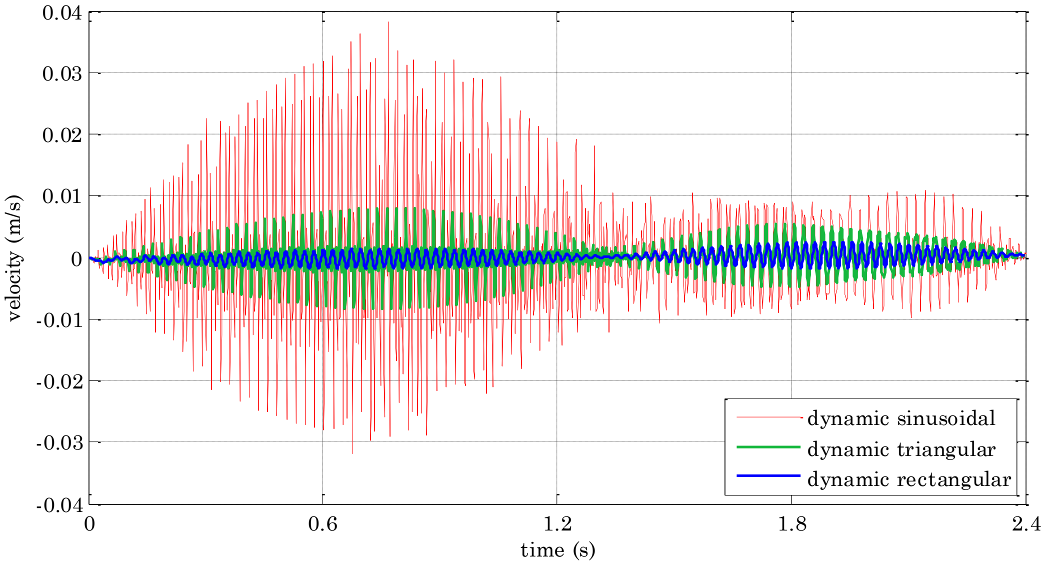

Figure 9. Dynamic responses of velocity in the mid-span

It is easy to see the beating phenomenon in nonlinear dynamic response of velocity, principally in rectangular form of irregularities, characterized by a rapid oscillation with a low amplitude variation due to superposition of waves with same direction, same amplitudes and nearby frequencies (Inman, 1996). All the dynamic responses of velocity vary between positive and negative values. The dynamic responses of velocity in rectangular irregularities, influenced by damage, have higher variations within the same time interval and major amplification of the oscillations.

The Figure 10 shows the dynamic responses of acceleration in the middle of the bridge.

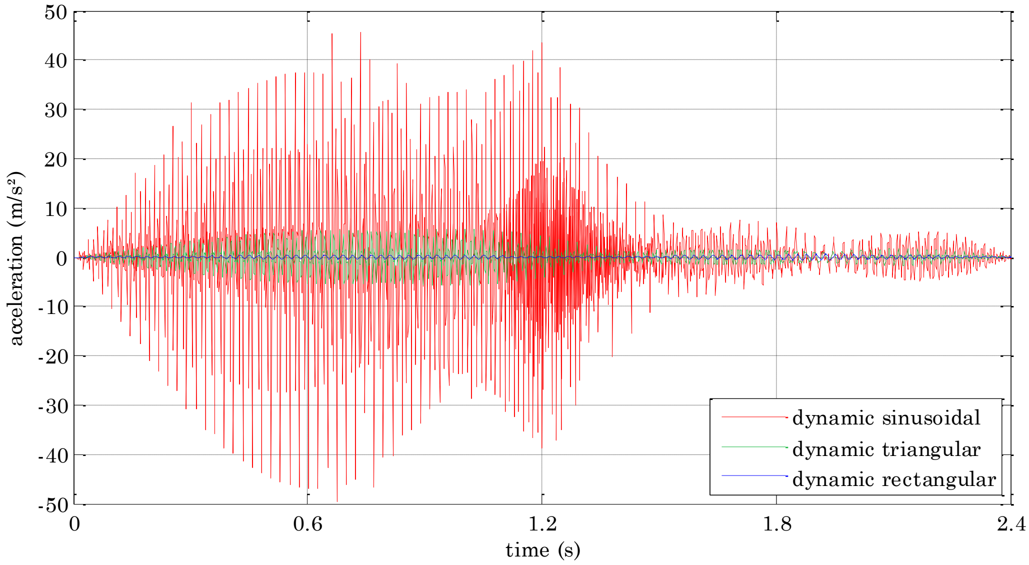

Figure 10. Dynamic responses of acceleration in the mid-span

The beating phenomenon can also be noted, indicated closeness to resonance. The dynamic responses of acceleration also vary between positive and negative values. The time response is coincident because the event is coincident, but there is great increase in the magnitude and the oscillations within the same time interval on the dynamic rectangular nonlinear responses due to damage. Although not intentionally emphasized, it is possible to observe the damping of the system.

The Figure 11 shows the damaged configuration of the bridge for the rectangular irregularities. There were no damage on triangular and sinusoidal analysis.

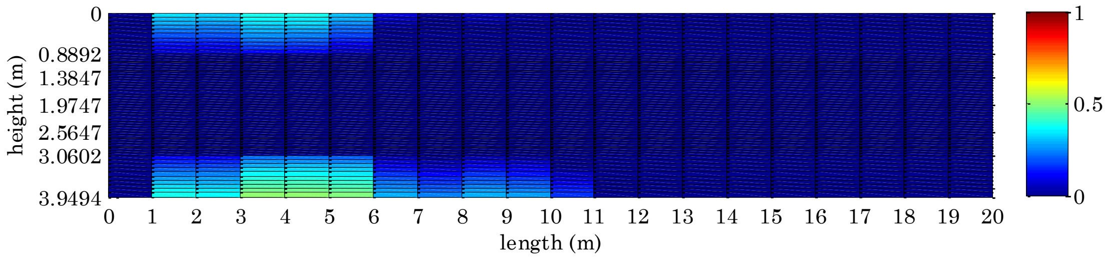

Figure 11. Damaged bridge configuration for the rectangular periodic irregularities

The longer duration of the amplitude from the rectangular irregularities, for the same period for all irregularities, causes the dynamic effects to be pontentiated resulting further damage to the bridge's structure. By analyzing the Figure 11 it can be noted that the fifth element is the most affected one during the damage process. Still, it is observed that the accumulated damage occurred near the first support. As the direction of the vehicle is from the right to the left, the larger dynamic effects occur early in the passage of the vehicle in the irregularities of the bridge for not having enough time to the structural damping action in attempting to stabilize the structure.

It is, therefore, interesting to observe the evolution of the damage in the most affected element, as shown in Figure 12.

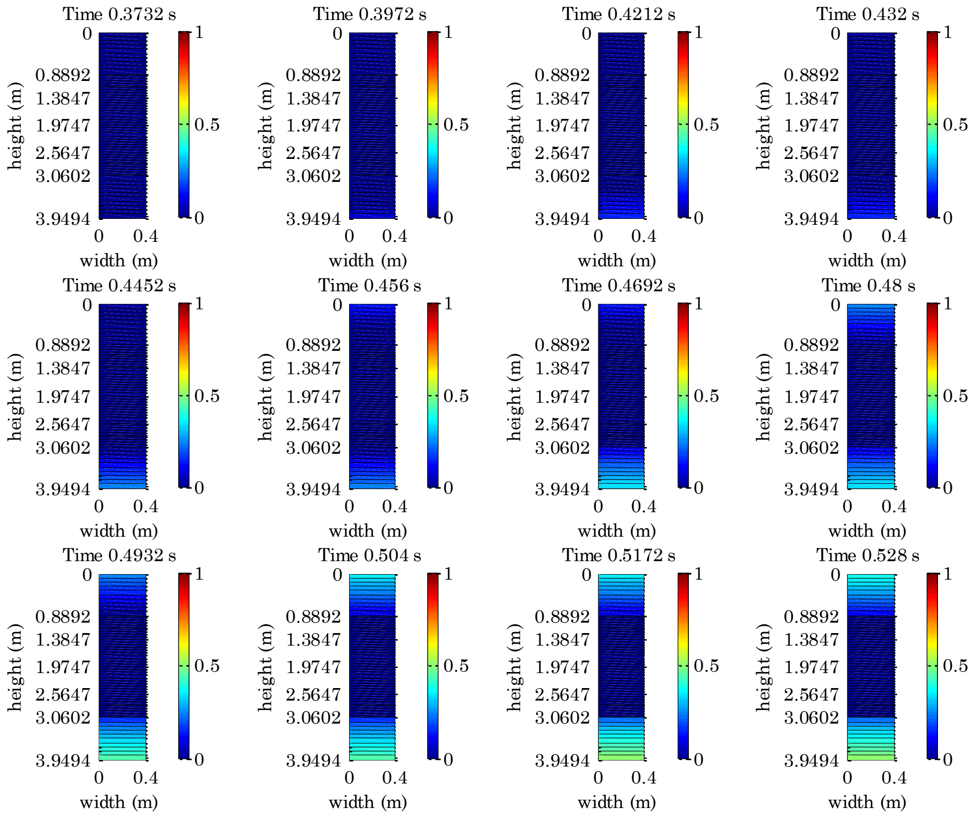

Figure 12. Damage evolution on the cross section of the most affected element through time

The evolution of damage takes place in early time steps. The damage evolved more on the distant layers because of the higher deformations these layers has. The damage that happened above and below the neutral axis, occurred by both traction and compression in both edges due to inversion of stresses due to vibration wherein commonly compressed upper layers become tractioned and vice versa. In an analysis that the stress inversion is not implemented such effect could not be detected.

Apart from changing the responses in terms of displacements, velocities and accelerations, the damage alters the natural frequencies of vibration of the structure. As the damage mechanics alters the stiffness of the bridge, the natural frequencies of vibration of the damaged bridge will be also penalized for being a relation between the stiffness and the mass of the structure.

The Table 3 below compares these frequencies obtained from the intact and the damaged bridge.

Table 3. Comparison between the natural frequencies of vibration of the intact and damaged bridge

Natural Frequencies of Vibration	Linear Dynamic Analysis (rad/s)	Nonlinear Dynamic Analysis of the Rectangular Irregularity (rad/s)
1st	46.1536860	45.4980275
2nd	184.7522534	181.1574457
3rd	415.9657361	407.8897178
4th	739.9920084	727.3316067
5th	1157.0654037	1135.0442653
6th	1667.5116640	1636.5849973
7th	2271.8006588	2231.7063230

The natural frequencies of vibration obtained from the damaged bridge are smaller than that obtained from the intact bridge. In this sense, it may be possible, in future works, to locate a fissure or its contained region by measures of the natural frequencies of vibration from a damaged bridge through accelerometers.

9 CONCLUSIONS

The linear dynamic analysis without considering the bridge's cross section is not effective to represent all the cases of dynamic interaction between vehicle, irregularities and bridge, as the exemplified case.

The dynamic responses of displacement were greater for the rectangular forms of irregularities and the greatest in the presence of damage. The rectangular waves are the most prone to inflict damages on the structure. There is no damage in sinusoidal and triangular analysis because the duration of the peak amplitude is much smaller than the rectangular forms of irregularities.

There were huge variations in nonlinear dynamic responses of velocity and acceleration within the same time interval, especially in rectangular irregularities. On these, the damage greatly increased the amplitude and oscillations of the responses.

The routine considering the cross section's geometry were capable to represent the dynamic responses of the structure in both linear and nonlinear cases, even capable to identify the damage evolution.

Acknowledgements

The first author would like to gratefully and sincerely thank all the other authors and all the teachers and staff of PPGEM/PUCPR, also acknowledge the financial support provided by CAPES.

REFERENCES

Abeche, T. de O., Machado, R. Dalledone, Beghetto, F. L. M., Souza, L. A. F., 2015. Computational modeling of vehicle-irregularity-bridge dynamic interaction by damage mechanics. In: 1st Pan American Congress on Computational Mechanics in conjunction with the XI Argentine Congress on Computational Mechanics, 2015, Buenos Aires, Argentina. Barcelona, Spain: *International Center for Numerical Methods in Engineering (CIMNE)*, v. 1. pp. 485-496.

Bathe, K. J., 1996. *Finite Element Procedures*. Prentice-Hall, New Jersey.

Chopra, A. K., 1995. *Dynamics of Structures: Theory and Applications to Earthquake Engineering*. Englewood Cliffs: Prentice Hall.

Inman, D. J., 1996. *Engineering Vibration*. Prentice-Hall, New-Jersey.

Jacob, B. P. & Ebecken, N. F. F., 1994. An optimized implementation of the Newmark/Newton-Raphson algorithm for the time integration of non-linear problems. *Communications in Numerical Methods in Engineering*, 10, pp. 983-992.

Kwon, Y. W. & Bang, H., 2000. *The Finite Element Method Using MATLAB*, 2nd edition, CRC Mechanical Engineering Series, CRC Press.

Lemaitre, J. & Chaboche, J. C., 1985. *Mécanique des matériaux solids*. Paris, Dunod-Bordas.

Lemaitre, J. & Desmorat, R., 2005. *Engineering Damage Mechanics: Ductile, Creep, Fatigue and Brittle Failures*. Springer-Verlag, Londres.

Machado, R. Dalledone, 1983. *Análise dinâmica não-linear de sistemas rígido-flexíveis*. Master's Dissertation, Instituto Alberto Luiz Coimbra de Pós-Graduação e Pesquisa de Engenharia (COPPE), Universidade Federal do Rio de Janeiro (UFRJ), Rio de Janeiro, RJ.

Mazars, J., 1984. *Aplication de la mécanique de l'endommagement au comportament non lineare et à la rupture du béton de structure*. Thése de Doctorat d'État, Université Paris 6, Paris.

Pasa, V. F., 2007. *Análise do Comportamento de Estruturas de Concreto Reforçado com Fibras de Aço via Método dos Elementos Finitos*. Master's Dissertation – Programa de Pós-Graduação em Engenharia Civil da Universidade Federal do Rio Grande do Sul, Porto Alegre, RS.

Pituba, J. J. C., 1998. *Estudo e aplicação de modelos constitutivos para o concreto fundamentados na Mecânica do Dano Contínuo*. Escola de Engenharia de São Carlos, Universidade de São Paulo, São Carlos.

Pituba, J. J. C. and Proença, S. P. B., 2005. Estudo e aplicação de modelos constitutivos para o concreto fundamentados na mecânica do dano contínuo. *Cadernos de Engenharia de Estruturas*, vol. 7, n. 23, pp. 33-60.

Rabotnov, Y. N., 1969. *Creep problems in structural members*. Amsterdam, North-Holland.

Tiago, C. M., Leitão, V. M. A. and Rosca, V., 2002. Análise de problemas unidimensionais de mecânica do dano com funções de base radial. J. M. Goicolea, C. Mota Soares, M. Pastor e G. Bugeda, Editor, *Métodos Numéricos en Ingeniería V*, Artes Gráficas Torres S.A.

Yang, Y. B., Yau, J. D., & Hsu, L. C., 1997. Vibration of simple beams due to trains moving at high speeds. *Engineering Structures*, Great Britain, v. 19, n. 11, pp. 936-944.